PHYSICAL REVIEW B VOLUME 11, NUMBER 4 15 FEBRUARY 1975

Hot-electron intervalley transfer in silicon

J. P. Nougier, M. Rolland, and D. Gasquet

Université des Sciences et Techniques du Languedoc, Centre d'Etudes d'Electronique des Solides, associé au Centre National de la Recherche Scientifique, 34060 Montpellier Cedex, France

(Received 29 July 1974)

Using symmetry considerations developed in a previous paper it is shown that, assuming ellipsoidal parabolic band structure, the populations of the valleys as a function of electric field intensity $\vec{E}$ can be deduced from drift-velocity measurements when $\vec{E}$ lies in the (110) plane. This is, as we know, the first direct determination of the transfer rate $r(E)$ of electrons between valleys, which does not involve any hypothesis concerning the scattering mechanisms and the coupling constants. $r(E)$ is plotted versus E for different lattice temperatures and impurity concentrations when $\vec{E} \| [100]$ and $\vec{E} \| [110]$ crystallographic directions. It is shown that the depopulation of the "hot" valleys reaches 50% at 77°K for $\vec{E} \| [100]$, and is a decreasing function of the lattice temperature and of the impurity concentration. Ninety percent of the drift-velocity anisotropy is due to intervalley transfer. At very high electric fields the carriers are again equipartitioned among the valleys. At low temperature the "hot" valleys become almost empty in a range of electric fields and this produces negative differential mobility.

I. INTRODUCTION

Experimental evidence of drift-velocity anisotropy in many-valley semiconductors in the hot-carrier range has been found by many workers.[1–4] This anisotropy was found to be partly produced by intervalley scattering. Very few computations of intervalley transfer rate have been performed. Some of them use the assumption of a displaced Maxwellian distribution function,[5–9] which has been proved to be a crude approximation, valid only for a few materials in a narrow range of temperatures and electric fields. Other calculations deal with a numerical resolution of the Boltzmann equation using a Monte Carlo technique[10]: these computations require knowledge of the scattering matrix, which introduces errors since some interactions are often neglected and the coupling constants are not well known.

The purpose of this paper is to determine the proportion of electrons lying in the valleys of silicon, deduced from drift-velocity measurements, using the crystal symmetries and assuming parabolic ellipsoidal valleys, without any hypothesis concerning the scattering mechanisms. In Sec. II, theoretical expressions for drift velocity will be deduced from symmetry considerations. Comparison with experimental data will give the populations of valleys when the electric field lies along a [100] direction (Sec. III) and along a [110] direction (Sec. IV) for different temperatures and carrier concentrations.

II. DRIFT VELOCITY FOR SEMICONDUCTORS WITH PARABOLIC ELLIPSOIDAL VALLEYS

A. General features

Symmetry considerations bring important information concerning the mobility tensor in the hot-electron range. It has been shown[1] quite generally that in cubic semiconductors only two components of the mobility tensor are independent. For semiconductors with parabolic ellipsoidal valleys, the drift velocity $\vec{v}(\vec{E})$ is the sum of each valley contribution, that is[1]

$$\vec{v}(\vec{E}) = \sum_i \frac{n_i(\vec{E})}{N} \vec{v}_i(\vec{E}) = \sum_i \frac{n_i(\vec{E})}{N} a_i(\vec{E}) \underline{m}_i^{-1} \vec{E} , \quad (1)$$

where N is the total density of carriers, index i refers to the valley number i, $\vec{v}_i(\vec{E})$ is the drift velocity of the $n_i(\vec{E})/N$ carriers lying in the ith valley. $\underline{m}_i^{-1}$ is the reciprocal effective-mass tensor and $a_i(\vec{E})$ a scalar which involves scattering processes. $a_i(\vec{E})$ may be written[1]

$$a_i(\vec{E}) = a(E^2 - E_i^2, E_i^2) , \quad (2)$$

where E is the electric field intensity and E_i is the component of $\vec{E}$ along the symmetry axis of valley number i. Each ellipsoidal valley can be transformed into a spherical one[11]: if the subscript ξ means any principal direction of the ith valley along which the effective mass is m_ξ, one gets:

$$\vec{v}_i^*(\vec{E}^*) = \mu^*(E^{*2}) \cdot \vec{E}^* , \quad (3)$$

where

$$v_{i\xi}^* = (m_\xi/m_0)^{1/2} v_{i\xi} , \quad (4)$$

$$E_\xi^* = (m_0/m_\xi)^{1/2} E_\xi . \quad (5)$$

m_0 is the electron mass, and $\mu^*(E^{*2})$ is a scalar. $\vec{v}_i^*(\vec{E}^*)$ can be derived from Eq. (1) using Eqs. (4) and (5). Identification with Eq. (3) then gives

$$a_i(\vec{E}) = a_i(E^{*2}) = a_i\left(\sum_\xi \frac{m_0}{m_\xi} E_\xi^2\right) , \quad (6)$$

that is

$$a_i(\vec{E}) = a[(m_0/m_t)(E^2 - E_i^2) + (m_0/m_l)E_i^2] , \quad (7)$$

where m_t and m_l are transverse and longitudinal effective masses.

It must be noticed that the distribution function $f_i(\vec{k}, \vec{E})$ of the carriers in the ith valley depend on that of the jth valley, through scattering which may produce intervalley transfer of carriers. However, the stationary state in a field $\vec{E}$ is such that when a carrier jumps from valley i to valley j, another carrier jumps from valley j to valley i, so that the population $n_i(\vec{E})/N$ of each valley remains unchanged, neglecting fluctuations. Therefore, as regards drift velocity, each valley behaves as if it were independent from other valleys, so that the total drift velocity is the sum of the contributions of each valley, and each valley can be transformed into a spherical one, which leads to Eqs. (1)–(7).

Contrary to what was said in Eq. (10) of Ref. 1, $n_i(\vec{E})$ has not the same form as $a_i(\vec{E})$ since it is not invariant in rotation with respect to the ith valley axis. For example in n-type silicon when $\vec{E}$ lies along a [111] direction, all the valleys are equivalent and $n_i(\vec{E})/N = \frac{1}{6}$, but after a rotation of $\vec{E}$ with respect to a [100] direction, the valleys are no more equivalent so that $n_i(\vec{E})/N \neq \frac{1}{6}$.

The symmetry properties of $n_i(\vec{E})$ in silicon can be deduced from considerations analogous to those developed in Ref. 1 and are given in the Appendix.

B. Case of *n*-type silicon

The mobility tensor in silicon was given in Ref. 1, where Eq. (17) must be slightly modified since $n_i(\vec{E})$ has not the same symmetry as $a_i(\vec{E})$. Hence the mobility tensor can be expressed using Eqs. (16) and (17) of Ref. 1 and Eq. (7) of the present paper:

$$\mu_{\alpha\beta}(\vec{E}) = \mu_{\alpha\alpha}(\vec{E})\delta_{\alpha\beta} ,$$

$$\mu_{\alpha\alpha}(\vec{E}) = \frac{2}{N}\sum_{\beta} \frac{n_\beta(\vec{E}) a[(m_0/m_t)(E^2 - E_\beta^2) + m_0/m_l\, E_\beta^2]}{m_l \delta_{\alpha\beta} + m_t(1 - \delta_{\alpha\beta})} \quad (8)$$

where $\delta_{\alpha\beta}$ is the Kronecker symbol, α and β are components along the crystallographic principal directions of silicon, and $n_\beta(E)$ is another notation for $n_i(E)$ since in silicon the valleys lie along the crystallographic principal directions.

When the electric field is applied along a [111] direction, all the valleys are equivalent, $n_\beta(\vec{E} \parallel \langle 111 \rangle)/N = \frac{1}{6}$, and the drift velocity is, following Eq. (8),

$$\vec{v}(\vec{E} \parallel \langle 111 \rangle) = \mu_{111}(E)\vec{E} , \quad (9)$$

where

$$\mu_{111}(E) = [(1 + 2\lambda)/3m_l] a[(m_0/m_l)\tfrac{1}{3}(1 + 2\lambda)E^2] \quad (10)$$

and

$$\lambda = m_l/m_t \quad (11)$$

for n-type silicon, $\lambda = 4.81$.[12] Equation (10) shows that measurement of $\mu_{111}(E)$ gives $a(E)$ as a function of electric field

$$a(E) = \frac{3m_l}{1 + 2\lambda}\, \mu_{111}\left(\frac{3m_l E}{m_0(1 + 2\lambda)}\right)^{1/2} . \quad (12)$$

III. ELECTRIC FIELD PARALLEL TO A [100] DIRECTION

A. Populations of the valleys

When

$$\vec{E} = (E, 0, 0) \quad (13)$$

the valleys are not equivalent. If $r_{100}(E)$ is the proportion of electrons leaving each valley perpendicular to $\vec{E}$, one gets, if indexes 1, 2, 3 refer to $\langle 100 \rangle$, $\langle 010 \rangle$, and $\langle 001 \rangle$ directions:

$$\frac{n_2(E, 0, 0)}{N} = \frac{n_3(E, 0, 0)}{N} = \frac{1 - r_{100}(E)}{6} , \quad (14)$$

$$\frac{n_1(E, 0, 0)}{N} = \frac{1 + 2r_{100}(E)}{6} . \quad (15)$$

These relations carried in Eq. (8) give

$$\vec{v}(\vec{E} \parallel \langle 100 \rangle) = \mu_{100}(E)\vec{E} , \quad (16)$$

where

$$\mu_{100}(E) = \frac{1}{3m_l}\left[[1 + 2r_{100}(E)]\, a\left(\frac{m_0}{m_l}E^2\right) + 2\lambda[1 - r_{100}(E)]\, a\left(\frac{m_0}{m_l}\lambda E^2\right)\right] . \quad (17)$$

Using Eq. (12), Eq. (17) gives

$$r_{100}(E) = \left\{\mu_{111}\left[\left(\frac{3}{1+2\lambda}\right)^{1/2} E\right] + 2\lambda\,\mu_{111}\left[\left(\frac{3\lambda}{1+2\lambda}\right)^{1/2} E\right] - (1 + 2\lambda)\,\mu_{100}(E)\right\} \Big/ 2\left\{\lambda\,\mu_{111}\left[\left(\frac{3\lambda}{1+2\lambda}\right)^{1/2} E\right] - \mu_{111}\left[\left(\frac{3}{1+2\lambda}\right)^{1/2} E\right]\right\} . \quad (18)$$

This shows that the anisotropy observed is due to the difference between longitudinal and transverse effective masses, since if $\lambda = 1$ Eqs. (17) and (12) lead to $\mu_{100}(E) = \mu_{111}(E)$. At low field, $\mu_{111} = \mu_{100} = \mu_0$ Eq. (18) then gives $r_{100} = 0$.

The experimental determination of $\mu_{111}(E)/\mu_0$ and $\mu_{100}(E)/\mu_0$ gives $r_{100}(E)$ at every electric field using Eq. (18). Experiments were performed at different temperatures on samples of various carrier concentration, using Ohmic contacts prepared following a method similar to that described elsewhere for p-type germanium.[13] A pulse bridge was used[14] for conductivity measurements with good accuracy. Figure 1 shows, as an example, mobilities versus electric field at 77 °K along [111] and [100] direc-

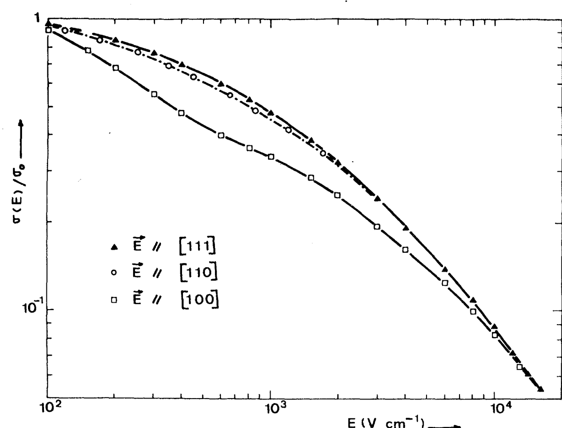

FIG. 1. Relative conductivity vs electric field at 77 °K for a n-type silicon sample of room-temperature resistivity $\rho_{300\,°K} = 15\ \Omega\,\mathrm{cm}$.

tions for a sample of room-temperature resistivity $\rho_{300} = 15\ \Omega\,\mathrm{cm}$. Figure 2 shows variations of $r_{100}(E)$ vs E at different temperatures, deduced from drift-velocity measurements performed by Canali *et al.*[15] on high-purity samples (ρ_{300} lying between 30 and 200 kΩ cm). E_c is the characteristic field defined as

$$E_c = v_{s\,111}/\mu_0\ , \qquad (19)$$

where μ_0 is the Ohmic mobility and $v_{s\,111}$ the drift velocity saturation along a [111] direction. E_c values are given in Table I. It can be seen that the transfer rate increases with increasing electric field, and reaches a maximum value r_{max} for a field not very far from E_c. At higher electric fields, the carriers in the longitudinal "cold" valleys become hot enough to be scattered again towards the "hot" valleys, $r(E)$ diminishes, and equipartition of

TABLE I. Values of characteristic field $E_c = v_{s111}/\mu_0$ in V cm^{-1} for various temperatures and carrier concentrations.

	77 °K	160 °K	300 °K
High purity (Canali *et al.*, Ref. 15)	635	2170	6600
$\rho_{300} = 15\ \Omega\,\mathrm{cm}$	870	2550	···
$\rho_{300} = 6\ \Omega\,\mathrm{cm}$	1110	3000	···

the carriers among the valleys occurs again at very high electric fields.

It can be noticed that r_{max} increases with decreasing temperature and reaches 0.54 at 77 °K. Then the concentration in the longitudinal valleys reaches twice the Ohmic concentration. Figure 3 shows $r_{100}(E)$ vs E at 77 °K for different carrier concentrations; it can be seen that the transfer rate diminishes as the carrier concentration increases, since carrier-carrier and carrier-impurity scattering enhances equipartition. These results are summarized in Tables I and II.

It is interesting to study the transfer rate when negative differential mobility (NDM) occurs. Such a phenomenon could not have been measured by the authors with the technique used on doped samples because it takes place at low temperature and then the carrier concentration does not remain constant because of impact ionization of impurities. NDM in n-type silicon has been observed on lightly doped samples[16,17] and on high-purity samples.[18] Figure 4 shows $r_{100}(E)$ deduced from experimental drift-velocity curves obtained at 8 °K and recently published by Reggiani *et al.*[19] Figure 4 clearly shows that NDM is due to strong depopulation of the val-

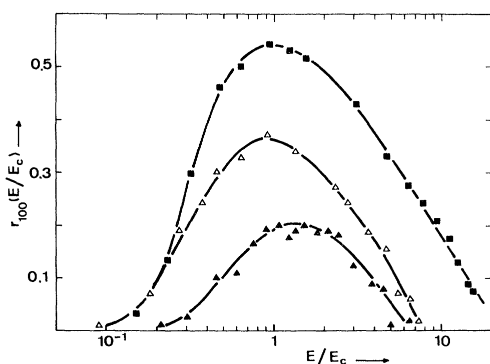

FIG. 2. Variations of $r_{100}(E)$ vs E/E_c at different temperatures for n-type silicon high-purity samples, deduced from drift-velocity measurements of Canali *et al.*,[15] ■, $T = 77\,°K$ ($E_c = 635$ V cm^{-1}); △, $T = 160\,°K$ ($E_c = 2160$ V cm^{-1}); ▲, $T = 300\,°K$ ($E_c = 6620$ V cm^{-1}).

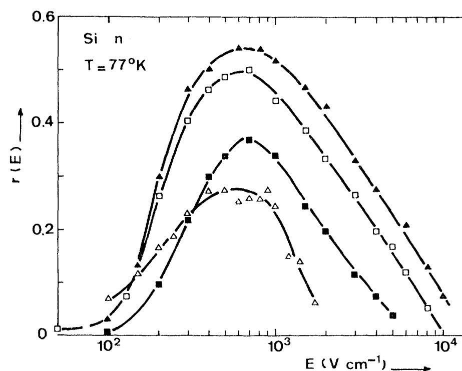

FIG. 3. Variation of $r_{100}(E)$ and $r_{110}(E)$ vs E at 77 °K for n-type silicon samples of various impurity concentrations. ▲, $r_{100}(E)$ for high-purity sample of Canali *et al.*[15]; □, $r_{100}(E)$ for $\rho_{300\,°K} = 15$-Ω cm sample ($E_c = 870$ V cm^{-1}); ■, $r_{100}(E)$ for $\rho_{300\,°K} = 6$-Ω cm sample ($E_c = 1170$ V cm^{-1}); △, $r_{110}(E)$ for $\rho_{300\,°K} = 6$-Ω cm sample.

TABLE II. Maximum rate transfer r_{max} for various temperatures and carrier concentrations, when $\vec{E} \parallel \langle 100 \rangle$.

	77 °K	160 °K	300 °K
High purity (Canali *et al.*, Ref. 15)	0.54	0.36	0.20
$\rho_{300} = 15\ \Omega$ cm	0.50	0.29	···
$\rho_{300} = 6\ \Omega$ cm	0.37	0.28	···

leys transverse to the electric field. When these are almost empty ($r_{max} \simeq 1$) the carriers are being scattered back in these valleys and the drift velocity along a [100] direction increases again. It must be noted that r_{max} exceeding 1 is due to imprecision of numerical values deduced from drift-velocity curves of Ref. 19. In any case, it can be easily shown from Eq. (18) that errors of 5% on drift-velocity measurements bring error of about 10% on r_{max}.

B. Anisotropy due to the crystal structure

The drift-velocity anisotropy is due to electron transfers between valleys as well as to the cubic symmetry and the difference between m_l and m_t. In order to compare the contributions of these phenomena, let us suppose that there is no electron transfer that is $r_{100}(E) = 0$. Equation (18) then gives

$$\mu_{100}(E) = \frac{1}{1+2\lambda}\left\{\mu_{111}\left[\left(\frac{3}{1+2\lambda}\right)^{1/2} E\right] + 2\lambda\mu_{111}\left[\left(\frac{3\lambda}{1+2\lambda}\right)^{1/2} E\right]\right\} . \tag{20}$$

From experimental determination of $\mu_{111}(E)$, Eq. (20) shows the variation of $\mu_{100}(E)$ vs E which would take place if no intervalley transfer could occur. The result is that $\mu_{100}(E)$ is then at most only 5% lower than $\mu_{111}(E)$, which shows by comparison with experimental variation of $\mu_{100}(E)$ that almost all the anisotropy is due to intervalley transfer, for example, in Fig. 1 at $E = 600\ \mathrm{V\,cm^{-1}}$ one obtains $\mu_{111} = 0.6\ \mu_0$ and $\mu_{100} = 0.4\mu_0$. If no intervalley transfer would occur, μ_{100} value would be $0.58\ \mu_0$, which shows that 90% of the anisotropy is due to intervalley transfer.

C. Drift-velocity saturation

At very high electric fields

$$v_{111}(E \to \infty) = v_{s111} , \tag{21}$$

and $r_{100}(E) = 0$ as was noted in Sec. III A. Equation (20) then gives, replacing $\mu_{111}(E)$ by v_{s111}/E,

$$\mu_{100}(E \to \infty) = \frac{1 + 2(\lambda)^{1/2}}{[3(1+2\lambda)]^{1/2}}\,\mu_{111}(E \to \infty) , \tag{22}$$

which shows that $v_{100}(E \to \infty)$ tends towards a saturation value v_{s100},

$$v_{s100} = 0.95\, v_{s111} . \tag{23}$$

Our experimental results as well as those of Canali *et al.*[15] gave $v_{s100} = v_{s111}$, which is due to experimental errors of about 5% at high field, which yields large errors for $r_{100}(E)$ because the denominator of Eq. (18) is then small. It can be shown from Eq. (18) that in the saturation range the uncertainty on $r_{100}(E)$ is

$$\Delta r_{100}(E) = 4.5\Delta\mu_{111}(E)/\mu_{111}(E) . \tag{24}$$

IV. ELECTRIC FIELD PARALLEL TO A [110] DIRECTION

The statement is the same as in Sec. III. Thus

$$\vec{E} = (E/\sqrt{2}, E/\sqrt{2}, 0) \tag{25}$$

and, if $r_{110}(E)$ is as previously the proportion of carriers leaving the hot valleys

$$\frac{n_1(E/\sqrt{2}, E/\sqrt{2}, 0)}{N} = \frac{n_2(E/\sqrt{2}, E/\sqrt{2}, 0)}{N} = \frac{1 + \frac{1}{2} r_{110}(E)}{6} ,$$
$$\frac{n_3(E/\sqrt{2}, E/\sqrt{2}, 0)}{N} = \frac{1 - r_{110}(E)}{6} . \tag{26}$$

Equations (25) and (26) substituted into Eq. (8) then give, taking into account Eq. (10),

$$\vec{v}(\vec{E} \parallel \langle 110 \rangle) = \mu_{110}(E)\vec{E} , \tag{27}$$

$$r_{110}(E) = 2\left\{\lambda\mu_{111}\left[\left(\frac{3\lambda}{1+2\lambda}\right)^{1/2} E\right] + (1+\lambda)\mu_{111}\left[\left(\frac{3(1+\lambda)}{2(1+2\lambda)}\right)^{1/2} E\right] - (1+2\lambda)\mu_{110}(E)\right\} \times \left\{2\lambda\mu_{111}\left[\left(\frac{3\lambda}{1+2\lambda}\right)^{1/2} E\right] - (1+\lambda)\mu_{111}\left[\left(\frac{3(1+\lambda)}{2(1+2\lambda)}\right)^{1/2} E\right]\right\}^{-1} . \tag{28}$$

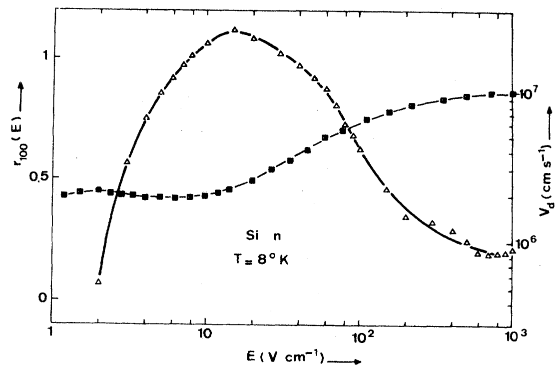

FIG. 4. Variation vs E at 8 °K for n-type silicon high-purity sample of ■, $r_{100}(E)$: experimental result of Reggiani *et al.*[19]; △, $r_{100}(E)$ deduced from Eq. (18) and experimental drift-velocity measurements of Reggiani *et al.*[19]

It has been noticed by several authors[4] that the longitudinal anisotropy is greater in a [100] direction than in a [110] direction (see also Fig. 1). However, $r_{110}(E)$ deduced from experimental results and Eq. (28) shows (see Fig. 3) that intervalley transfers are comparable for $\vec{E} \parallel [100]$ and $\vec{E} \parallel [110]$. At high electric fields, $r_{110}(E) = 0$ and $\mu_{111}(E) = v_{s111}/E$, Eq. (28) then gives

$$\mu_{110}(E \to \infty) = 0.99 \mu_{111}(E \to \infty) . \quad (29)$$

This result compared to Eq. (23) as well as Fig. 3 shows that the anisotropy diminution is not due to difference between intervalley transfers but to the crystal structure and differences between m_l and m_t. However it must be noted that for a given depopulation of the hot valleys, the cold valleys become much more populated when $\vec{E}$ lies along a [100] direction than when $\vec{E}$ lies along a [110] direction.

V. CONCLUSION

The mobility tensor symmetries recently studied in the hot carrier range for cubic semiconductors[1] have been applied in this paper to the case of n-type silicon with the additional hypothesis of ellipsoidal parabolic valleys. The populations of the valleys were deduced from drift-velocity measurements: this is, as we know, the first direct determination of the populations which does not involve any hypothesis concerning the scattering mechanisms and the coupling constants. It has been shown that intervalley transfer increases with electric field, reaches a maximum value when E is to the order of magnitude of E_c, and then decreases at higher field. The maximum depopulation rate r_{max} of the "hot" valleys reaches 50% at 77 °K and 100% at 8 °K for pure silicon when $\vec{E}$ lies along a [100] direction and r_{max} is a decreasing function of lattice temperature and carrier concentration. This method applied for $\vec{E} \parallel [100]$ and $\vec{E} \parallel [110]$ can be used for any direction of $\vec{E}$ such as when the conduction involves two groups of equivalent valleys; this is the case in n-type silicon for $\vec{E}$ located in the (110) crystallographic plane.

ACKNOWLEDGMENT

The authors are much indebted to Professor M. Savelli for helpful discussions.

APPENDIX: SYMMETRY RELATIONS FOR $n_i(\vec{E})$

S_0 being the symmetry with respect to the (001) plane, and $n_i(\vec{E})$, $n_2(\vec{E})$, $n_3(\vec{E})$ the number of carriers lying along the ⟨100⟩, ⟨010⟩ and ⟨001⟩ crystallographic directions, one gets

$$n_i(S_0 \vec{E}) = n_i(\vec{E}) ,$$

where $i = 1, 2, 3$ and

$$\vec{E} = (E_1, E_2, E_3) ,$$
$$S_0\vec{E} = (E_1, E_2, -E_3);$$

this shows that $n_i(\vec{E})$ is an even function of each component E_j. Let S_b be the symmetry with respect to the first bisector plane:

$$n_1(S_b\vec{E}) = n_2(\vec{E}) ,$$
$$n_2(S_b\vec{E}) = n_1(\vec{E}) ,$$
$$n_3(S_b\vec{E}) = n_3(\vec{E}) ,$$

which gives

$$\left.\begin{matrix} E_i \rightleftarrows E_j \\ E_k \rightleftarrows E_k \end{matrix}\right\} \Rightarrow \left\{\begin{matrix} n_i \rightleftarrows n_j \\ n_k \rightleftarrows n_k \end{matrix}\right. .$$

Let R be a $\frac{1}{3}2\pi$ rotation with respect to a [111] direction. A circular permutation of the $\vec{E}$ components gives a circular permutation on n_1, n_2, n_3. Finally, if $\vec{n}(\vec{E})$ is a vector defined as

$$\vec{n}(\vec{E}) = (n_1(\vec{E}), n_2(\vec{E}), n_3(\vec{E})) ;$$

the above results may be written

$$\vec{n}(S_0\vec{E}) = \vec{n}(\vec{E}) ,$$
$$\vec{n}(S_b\vec{E}) = S_b\vec{n}(\vec{E}) ,$$
$$\vec{n}(R\vec{E}) = R\vec{n}(\vec{E}) .$$

[1]J. P. Nougier, Physica (Utr.) 62, 565 (1972).
[2]E. G. S. Paige, *Progress in Semiconductors* (Heywood, London, 1964), Vol. 8.
[3]E. M. Conwell, Solid State Phys. Suppl. 9, 49 (1967).
[4]M. Asche and O. G. Sarbei, Phys. Status Solidi 33, 9 (1969).
[5]M. Asche, B. L. Boichenko, and O. G. Sarbei, Phys. Status Solidi 9, 323 (1965).
[6]E. G. S. Paige, Proc. Phys. Soc. Lond. B 75, 174 (1960).
[7]W. E. K. Gibbs, J. Phys. Chem. Solids 25, 247 (1964).
[8]M. I. Nathan, Phys. Rev. 130, 2201 (1963).
[9]M. Costato and L. Reggiani, Phys. Status Solidi 42, 591 (1970).
[10]W. Fawcett, A. D. Boardman, and S. Swain, J. Phys. Chem. Solids 31, 1963 (1970).
[11]C. Herring and E. Vogt, Phys. Rev. 101, 944 (1956).
[12]J. C. Hensel, Phys. Rev. A 138, 225 (1965).
[13]J. P. Nougier and M. Rolland, Solid-State Electron. 16, 1399 (1973).
[14]J. P. Nougier, J. Comallonga, and M. Rolland, J. Phys. E 7, 287 (1974).
[15]C. Canali, G. Ottaviani, and A. Alberigi Quaranta, J. Phys. Chem. Solids 32, 1707 (1971).

[16]M. H. Jørgensen, N. O. Gram, and N. I. Meyer, Solid State Commun. 10, 337 (1972).
[17]N. O. Gram, Phys. Lett. A 38, 235 (1972).
[18]C. Canali, A. Loria, F. Nava, and G. Ottaviani, Solid State Commun. 12, 1017 (1973).
[19]L. Reggiani, S. Fontanesi, G. Ottaviani, and M. Costato, Second Symposium on the Physics of Plasma and Electrical Instabilities in Solids, Vilnius (SSSR) (1974), (unpublished).